Fractals, Vol. 3, No. 1 (1995) 161–181


8

# CHAOS AND FRACTALS AROUND BLACK HOLES

C. P. DETTMANN and N. E. FRANKEL
*School of Physics, University of Melbourne, Parkville Victoria 3052, Australia*
N. J. CORNISH
*Department of Physics, University of Toronto, Toronto, Ontario M5S1A7, Canada*

Received January 17, 1995; Accepted January 20, 1995

**Abstract**

Fractal basin boundaries provide an important means of characterizing chaotic systems. We apply these ideas to general relativity, where other properties such as Lyapunov exponents are difficult to define in an observer independent manner. Here we discuss the difficulties in describing chaotic systems in general relativity and investigate the motion of particles in two and three black hole spacetimes. We show that the dynamics is chaotic by exhibiting the basins of attraction of the black holes which have fractal boundaries. Overcoming problems of principle as well as numerical difficulties, we evaluate Lyapunov exponents numerically and find that some trajectories have a positive exponent.

## 1. INTRODUCTION

As we look out into the universe with ever more powerful telescopes, we begin to see that the structures formed through gravitational organization often have complicated, and sometimes fractal, geometry. The Voyager misson revealed Saturn's rings to have an intricate distribution of rings and voids, providing a fractal image of the underlying chaotic gravitational dynamics. A similarly produced series of gaps can be seen in the asteroid belt which lies between Mars and Jupiter.[1,2] Looking beyond our solar system, the large scale structure of the universe appears to be fractal over a range of scales,[3] and is commonly thought to be the result of chaotic evolution from smooth initial conditions. Furthermore, when describing the universe using Einstein's theory of gravity, space and time become dynamical and the evolution of spacetime itself can be chaotic due to the nonlinear nature of Einstein's equations.

In this paper we study test particle trajectories in multi-black hole spacetimes. We shall see that the phase space is divided into basins of attraction which are separated by a fractal boundary. The presence of fractal boundaries is due to the chaotic nature of the dynamics. It is no surprise that particle trajectories can be chaotic in general relativity since many-body Newtonian systems are known to be chaotic and Einstein's theory recovers Newtonian gravity for weak fields and small velocities. What is more surprising is the occurrence of chaotic attractors in a Hamiltonian system, a feature that is foreign to nonrelativistic celestial dynamics. Attractors can arise in relativistic systems since there is a finite maximum velocity, the speed of light, and even light can be captured by a strong gravitational field. In the multi-black-hole spacetime we shall study, the black holes act as attractors in phase space. In fact, the whole concept of what we mean by a phase space is fundamentally changed once we consider general relativity. In the Newtonian view of the universe space and time exist as a rigid underlying structure, providing a fixed reference frame with which positions and velocities can be unambiguously defined. In contrast, space and time are dynamical concepts in general relativity and the coordinate system we use to describe notions of time and place lose any fundamental significance. Thus it is important to describe the chaotic dynamics in terms which do not depend on the chosen coordinate system.

The outline of this paper is as follows. In Sec. 2 we discuss the subtle issues that must be confronted when attempting to quantify chaos and fractals in general relativity. In the following sections, we investigate the motion of neutral and charged test particles in the combined gravitational and electric fields of two or three black holes, following on from Refs. 4–7. Each black hole has charge equal to its mass, so that the total force between them is zero, and only the motion of the particle need be considered. This paper is the first major study of the fractal boundary basin and Lyapunov exponents of this system. In Sec. 3 we write down the metric corresponding to this situation, noting in passing that it is possible to write down exact solutions of the Einstein-Maxwell equations containing fractal singularities. The Hamilton-Jacobi method is used to show that the two-black-hole problem is integrable in the weak field limit. In Sec. 4 we look at qualitative features of this system which are characteristic of chaotic dynamics, such as sensitive dependence on initial conditions, complicated basin boundaries, and universality. The effect of changing the charge/mass ratio of the test particle and the mass of the black holes is considered, and the three-black-hole problem is also treated. Section 5 investigates quantitative indicators of chaos, that is, fractal dimensions and Lyapunov exponents.

## 2. CHAOS AND FRACTALS IN GENERAL RELATIVITY

Studies of chaos in general relativity fall broadly into two categories. Those in the first group look for chaos in the Einstein field equations. After a coordinate system has been chosen there are six nonlinear second order coupled partial differential equations, so drastic simplications are used to make analytic or numerical calculations tractable. The system receiving the most attention from the point of view of chaos has been the Mixmaster Universe.[8,9] This is a general cosmological model which is homogeneous but not isotropic. Einstein's equations in vacuum reduce to three second order ordinary differential equations with one constraint, thus reducing the dimension of the phase space from infinity to five. Even with this comparative simplicity, there has been much debate as to the existence and nature of chaos in this model. Most authors have concentrated on obtaining Lyapunov exponents (see Eq. (26) and surrounding discussion) of either the full equations[10–12] or discrete approximates.[13,14] The main difficulty is that time is a parameter in general relativity, with the same status as spatial coordinates, so there is no natural variable "t" to use in Eq. (26). Thus Lyapunov exponents which are nonzero with respect to the discrete time are zero with respect to the time variable in which the equations take their simplest form.[15] This difficulty is directly related to what is known as "the problem of time" in quantum cosmology.[16] Like chaos, quantum mechanics relies on a fixed notion of time to define evolution.

One approach to circumvent this difficulty has been to represent the dynamics as geodesic motion in a curved space. If the curvature is negative there is sensitive dependence on initial conditions and the dynamics may be chaotic.[17,18] Sensitivity to initial conditions is necessary for chaos, but not sufficient. Other conditions, such as a compact phase space and mixing of trajectories are required to prove that a system exhibits chaos.[19] This

method has the advantage that it is based on curvature scalars which do not depend on a choice of coordinate system; however, its applicability to the Mixmaster system has been questioned.[20] There has also been a study of the homoclinic loops of a Mixmaster Universe containing matter, albeit with an unrealistic equation of state.[21] To summarize, the study of chaos in the Mixmaster Universe has been hampered by a lack of suitable coordinate invariant quantities to characterize the dynamics. In contrast, a Robertson-Walker model (which is isotropic) containing a scalar field has been shown to exhibit chaotic behavior by other methods such as the use of Poincare sections, which contain coordinate independent information.[22]

The other class of general relativistic chaotic system, the one which will concern us, is the dynamics of particles interacting with a given gravitational and electromagnetic field configuration. Examples include particles in the gravitational and electrostatic fields of two or more black holes,[4–7] charged particles in a constant magnetic field interacting with gravitational waves,[23] particles near a black hole interacting with gravitational waves[24] and particles near a black hole immersed in a constant magnetic field.[25] The chaos in these systems has been investigated using methods borrowed from nonrelativistic systems: analysis of the periodic orbits,[4–6] Poincare sections,[5,23,25] Lyapunov exponents,[7,25] fractal dimensions,[7] the Chirikov criterion,[23] and the Melnikov method.[24] These methods were generalized to relativistic systems in a fairly straightforward manner (with the possible exception of Lyapunov exponents) because all of the above gravitational systems are either static or static with a small periodic perturbation, so there is a well-defined global time parameter, and the phase space is in some sense static. Lyapunov exponents are discussed in more detail below. For recent reviews of chaos in general relativity, for both the field equations and the motion of particles, we refer the reader to Ref. 26.

It would appear that fractals do not fit well with general relativity, as the former are essentially nondifferentiable, but general relativity is based on smooth manifolds as models for spacetime. Nevertheless there have been attempts to use a nondifferentiable manifold as a model for spacetime, either as resulting from quantum gravity, or in an attempt to explain the wavelike properties of elementary particles. This type of approach is difficult mathematically, and is far from providing a complete theory at present, although there are some encouraging results. A number of recent articles on this subject may be found in Ref. 27. In contrast, we show here that fractal basin boundaries provide a particularly reliable quantification of chaos in general relativity.

## 3. PARTICLES IN MULTI-BLACK-HOLE SPACETIMES

### 3.1 Formalism

In nonrelativistic classical mechanics gravity and electrostatics both have an inverse square force law, so that in any static distribution with equal mass and charge distributions (in appropriate units: $4\pi\varepsilon_0 = G = c = 1$) the gravitational and electrostatic forces cancel, and the distribution remains static.

Remarkably, the same situation holds in general relativity. Majumdar[28] and Papapetrou[29] independently showed that for the static metric:

$$ds^2 = -U^{-2}dt^2 + U^2(dx^2 + dy^2 + dz^2)\,, \qquad (1)$$

where $U$ is a function of the spatial coordinates, together with the electrostatic potential

$$A_t = U^{-1} \qquad (2)$$

the Einstein-Maxwell equations reduce to Laplace's equation:

$$\nabla^2 U(x, y, z) \equiv U_{,xx} + U_{,yy} + U_{,zz} = 0\,. \qquad (3)$$

Thus, as in nonrelativistic mechanics, there is a static solution of the field equations for every solution of Laplace's equation. Hartle and Hawking[30] gave physical interpretation to these solutions, showing that if $U$ is of the form:

$$U = 1 + \sum_{i=1}^{N} \frac{M_i}{\sqrt{(x - x_i)^2 + (y - y_i)^2 + (z - z_i)^2}}\,, \qquad (4)$$

the Majumdar-Papapetrou (MP) metric corresponds to a system of black holes with equal charge and mass $M_i > 0$ and horizons at $(x_i, y_i, z_i)$. Note that these points are coordinate singularities, that is, a single point in the MP coordinate system corresponds to a black hole horizon of finite proper area. Hartle and Hawking extended the coordinate system to include the region inside the black holes.

They also showed that for any other form of the solution containing points at which $U$ is infinite or zero, the singularity is real, and not a result of the coordinate system chosen. It is straightforward to use the MP metric to write down spacetime solutions corresponding to charged cosmic strings (of finite extent) or even fractal distributions of mass and charge.[31] A knowledge of these solutions enriches our understanding of the singularity structure of more generic solutions of the Einstein-Maxwell equations, although the status of naked singularities as realistic models of physical objects is doubtful at present.[32]

Recently the MP spacetimes have been generalized to include a positive cosmological constant.[33,34] These solutions describe coalescing extremal black holes in a de Sitter type universe. A possible generalization of this paper would be to investigate the motion of particles in these spacetimes. The main differences would be that the Ricci curvature is negative (leading to instability) and the spacetime is no longer static.

The general relativistic equation of motion for a particle of charge $e$ and mass $m$ in combined electromagnetic and gravitational fields is most simply derived from the super-Hamiltonian[35]:

$$\mathcal{H} = \frac{1}{2} g^{\mu\nu}(\pi_\mu - eA_\mu)(\pi_\nu - eA_\nu)\,, \tag{5}$$

where Hamilton's equations:

$$\frac{\partial \mathcal{H}}{\partial \pi_\mu} = \frac{dx^\mu}{d\lambda}\,, \qquad \frac{\partial \mathcal{H}}{\partial x^\mu} = -\frac{d\pi_\mu}{d\lambda}\,, \tag{6}$$

are written in terms of an affine parameter $\lambda$ related to the particle proper time by $\tau = m\lambda$. The mass shell constraint is:

$$\mathcal{H} = -\frac{m^2}{2}\,. \tag{7}$$

The first Hamilton equation relates the canonical momenta $\pi_\mu$ to the four-velocities:

$$g^{\mu\nu}(\pi_\mu - eA_\mu) = g^{\mu\nu} p_\mu = m u^\nu\,. \tag{8}$$

The second equation gives a generalized Lorentz force equation. In the MP metric the equations for the spatial components of the momentum reduce to:

$$\frac{dp_i}{d\lambda} = \frac{\partial U}{\partial x^i}\left(U p_0^2 + e p_0 + U^{-3} \sum_j p_j^2\right). \tag{9}$$

The equations may be simplified slightly by using the four-velocity in an orthonormal (as opposed to a coordinate) basis:

$$u^{\hat{0}} = -\frac{U p_0}{m}\,, \qquad u^{\hat{i}} = \frac{p_i}{Um}\,, \tag{10}$$

which has a straightforward physical interpretation: the components are simply $(\gamma, \gamma\mathbf{v})$ as measured by an observer stationary with respect to the spacetime. Writing the components $u^{\hat{i}}$ in vector notation as simply $\mathbf{u}$ and $u^{\hat{0}}$ as $\gamma$, and using a dot for derivatives with respect to proper time $\tau$, the equations become:

$$\dot{\mathbf{u}} = U^{-2}[(\gamma^2 + u^2 - e\gamma/m)\nabla U - \mathbf{u}\mathbf{u}\cdot\nabla U]\,, \tag{11}$$

$$\dot{\mathbf{x}} = U^{-1}\mathbf{u}\,, \tag{12}$$

$$\dot{t} = U\gamma\,, \tag{13}$$

$$\gamma = \sqrt{1+u^2}\,. \tag{14}$$

These equations are used in the numerical integration, described below. Because the equations are time-independent, there is a conserved energy, given by:

$$E = -\pi_0 = U^{-1}(m\gamma - e)\,. \tag{15}$$

The energy of the particle at infinity is given by $E+e$, rather than simply $E$, in order to account for the non-zero electromagnetic potential energy at infinity. Constancy of the energy is a useful check of the numerical results, since it is not enforced directly when evolving a trajectory.

### 3.2 Hamilton-Jacobi Method

Consider the two black hole system, described by the above equations of motion with the appropriate expression for $U$ from Eq. (4). Without loss of generality masses $M_1$ and $M_2$ are placed at $(0,0,1)$ and $(0,0,-1)$ respectively. We want to elucidate the structure of the dynamics and classify the problem as integrable or chaotic, and if it is chaotic, to understand the role of relativity in quantifying the chaos.

The Newtonian version of the two-black-hole system, that is, a particle moving in the field of two fixed masses, is integrable, and was first solved by Euler. It is instructive to see the effect of relativistic terms in this solution. The technique we will use is the Hamilton-Jacobi method (chapter 10 of Ref. 36), used by Carter to solve the equations for a

particle moving in the field of a single rotating black hole.[37] If the Hamilton-Jacobi equation for a particular problem is separable, the system is integrable (non-chaotic), and all of the constants of motion are obtained. Note that our previous short paper[7] uses different conventions for $E$, $\lambda$, $\mathcal{H}$ and the form of the Hamilton-Jacobi equation than those given below. Here, the conventions conform to the most common usage in the literature.

We begin by writing the Hamiltonian using the most natural coordinates for the system, which in this case are prolate spheroidal coordinates, used in previous studies[4–7,38]:

$$\begin{aligned} x &= \sinh\psi \sin\theta \cos\phi\,, \\ y &= \sinh\psi \sin\theta \sin\phi\,, \\ z &= \cosh\psi \cos\theta\,. \end{aligned} \tag{16}$$

The metric (1) becomes

$$\begin{aligned} ds^2 &= -U^{-2}dt^2 \\ &\quad + U^2(Qd\psi^2 + Qd\theta^2 + \sinh^2\psi \sin^2\theta d\phi^2)\,, \end{aligned} \tag{17}$$

where

$$\begin{aligned} &U=1+W/Q\,, \quad Q=\sinh^2\psi+\sin^2\theta\,, \\ &W=(M_1+M_2)\cosh\psi+(M_1-M_2)\cos\theta\,. \end{aligned} \tag{18}$$

The Hamilton-Jacobi equation is the partial differential equation for $S(x^\mu, \lambda)$ obtained by taking the equation $\mathcal{H} = -\partial S/\partial\lambda$ and replacing the momenta $\pi_\mu$ in $\mathcal{H}$ by $\partial S/\partial x^\mu \equiv S_{,\mu}$, that is,

$$\begin{aligned} -S_{,\lambda} = -\frac{U^2}{2}\left(S_{,t} - \frac{e}{U}\right)^2 + \frac{1}{2U^2Q}(S_{,\psi}^2 + S_{,\theta}^2) \\ + \frac{S_{,\phi}^2}{2U^2\sinh^2\psi\sin^2\theta}\,. \end{aligned} \tag{19}$$

The equation is solved by separation of variables, starting from an ansatz of the form:

$$S = \Lambda(\lambda) + T(t) + \Psi(\psi) + \Theta(\theta) + \Phi(\phi)\,. \tag{20}$$

Because $\lambda$, $t$, and $\phi$ are cyclic coordinates which do not appear in $\mathcal{H}$, there are three obvious constants of the motion, which give:

$$\Lambda = \frac{m^2\lambda}{2}\,, \quad T = -Et\,, \quad \Phi = L_z\phi\,. \tag{21}$$

Here, $L_z$ is the $z$ component of angular momentum. For the full two-black-hole geometry, the remaining equation does not separate, so no further constants of the motion may be found. However, in the weak field approximation, that is, to first order in $W/Q$, we substitute:

$$QU^n \approx Q + nW\,, \tag{22}$$

in the Hamilton-Jacobi equation, and it separates to obtain:

$$\begin{aligned} \Psi = \int\{&[4E^2 + 6eE + 2e^2 - 2m^2](M_1 + M_2)\cosh\psi \\ &+ [(E+e)^2 - m^2]\sinh^2\psi \\ &- L_z^2/\sinh^2\psi + \alpha\}^{1/2}d\psi\,, \end{aligned} \tag{23}$$

$$\begin{aligned} \Theta = \int\{&[4E^2 + 6eE + 2e^2 - 2m^2](M_1 + M_2)\cos\theta \\ &+ [(E+e)^2 - m^2]\sin^2\theta \\ &- L_z^2/\sin^2\theta - \alpha\}^{1/2}d\theta\,. \end{aligned} \tag{24}$$

This shows that the weak field approximation is integrable, with the final constant of the motion being the separation constant $\alpha$. There is a clear physical interpretation of this result: The non-relativistic problem is separable in prolate spheroidal coordinates because the ellipses and hyperbolae which constitute the lines of constant $\psi$ and $\theta$ are particle trajectories. But when the potential becomes of order unity, relativistic effects become important, including the well-known result that elliptic orbits precess. Note that we have not made any approximation about the velocity of the particle. A relativistic particle moving in a weak potential is only slightly deflected, and still does not exhibit chaos.

The above result says very little about the fully relativistic two-center problem, except that prolate spheroidal coordinates are not uniquely suited to studying this system, except from the point of view of the nonrelativistic limit. To determine whether the MP problem is chaotic, we must define parameters to quantify the chaos which arise naturally in the formalism of general relativity. The parameters we will use are fractal dimensions and Lyapunov exponents, evaluated numerically by integrating the equations of motion. It may be possible to prove the existence of chaos analytically; however, there is no general method for doing this in a given dynamical system.[39] A recent preprint[19] uses coordinate invariant criteria to study the motion of photons in MP spacetimes, and concludes that all periodic

orbits are unstable, but needs numerical results such as those given here to back up an argument that this system is chaotic.

Assuming that this system is chaotic, for which we give very strong numerical evidence below, the transition to chaos from the integrable Newtonian two center problem could then be investigated by writing the Hamiltonian as an integrable, weak field term and a small relativistic perturbation. As the strength of the perturbation is increased, the KAM tori of the integrable system are destroyed by phase space resonances[24,40] leading to stochastic layers, cantori, and so on. We use a more direct numerical approach here, and leave such an investigation to a future paper.

For three or more masses, the Newtonian system is chaotic, except in the trivial case of test particles with $e = m$, which experience no force at all. Relativistically, these particles do experience a force if they are moving, which is proportional to $v^2$ if $v \ll c$, so the dynamics is not trivial.

## 4. QUALITATIVE FEATURES

The equations of motion may be integrated using a 4th order Runge-Kutta routine with adaptive step size, similar to the one given in Ref. 41. The accuracy of the integration may be checked by a number of methods, including varying the step size controlling parameter, checking that energy is conserved, and making sure that the trajectories are physically reasonable.

The results in this and the following section are almost entirely for the two-black-hole problem, with masses of $1/3$, placed at $x = z = 0$, $y = \pm 1$, and a test particle of zero charge. A typical trajectory for this system is shown in Fig. 1. Note that, in contrast to the equivalent Newtonian system, there is a finite cross section for capture by one of the black holes. The numerical integration tests for this by stopping whenever the step size becomes smaller than a predefined limit.

A trajectory with similar initial conditions to the above trajectory is shown in Fig. 2. The outcome

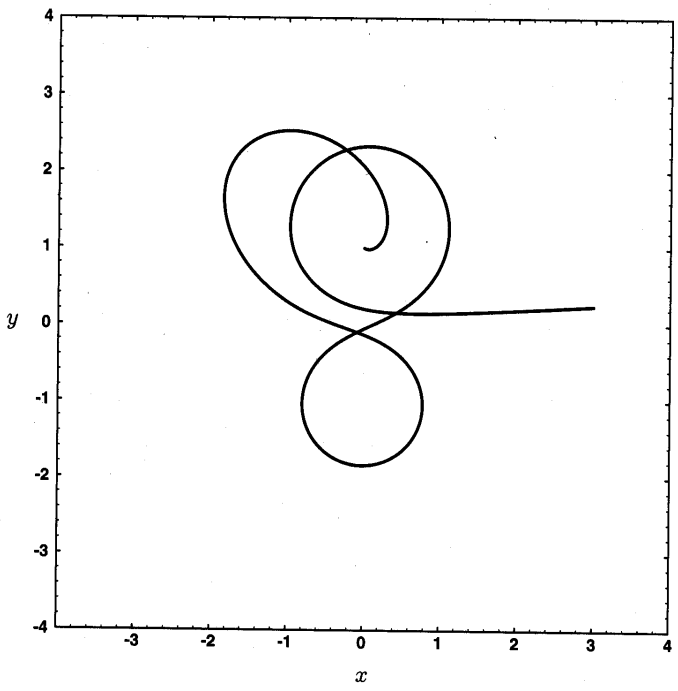


**Fig. 1** A trajectory with initial conditions ($x = 3$, $y = 0.249$, $u_x = 0$, $u_y = 0$).

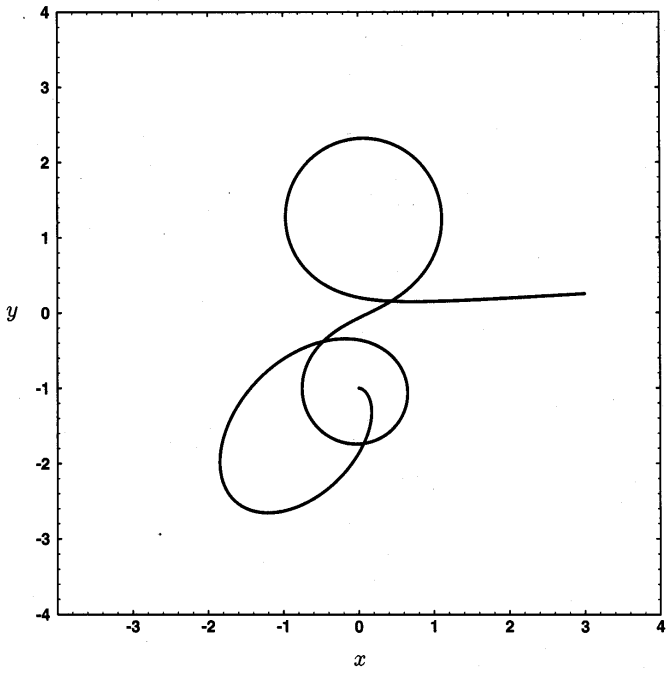


**Fig. 2** A trajectory with initial conditions ($x = 3$, $y = 0.25$, $u_x = 0$, $u_y = 0$).

is quite different: the particle ends up in the other black hole. These trajectories are not particularly special, but the outcome depends sensitively on the initial conditions. This characteristic of the dynamics is one of the effects of chaos.

Not all trajectories end up in one of the black holes. Even for trajectories with negative energy, which cannot escape to infinity, the particle may orbit indefinitely. An example of this is shown in Fig. 3. The phase space may thus be divided into three sets, the basin of attraction of the black hole at $y = 1$, which is marked in black in the following figures; the basin of attraction of the black hole at $y = -1$, which is marked in white; and those trajectories which continue to infinite proper time, which are marked in grey. Numerically, it is only possible to integrate to a finite proper time; however, it is found that trajectories which fall into one of the black holes do so within a few orbits. That is, varying the maximum time cutoff has virtually no effect on the results, after about 1000 (proper) time units.

Some $\mathbf{u} = 0$ slices of phase space are shown in Figs. 4–8. It is seen that the basins of attraction are quite complicated, and their mutual boundary appears to be a fractal. This is another indication that this system is chaotic. We will quantify the fractal nature of this section of the basin boundary in the next section by obtaining a numerical estimate of its dimension.

Figure 8 contains a grey region. As noted above it is not possible to prove that the trajectories in this region survive for infinite time; however, the picture does not change much if the maximum time is increased, so this looks to be a real effect. A typical trajectory in this region is shown in Fig. 9. The particle starts at rest at one end of the trajectory, moves to the other end, and then retraces its steps. This orbit is stable, otherwise numerical errors would cause it to deviate after a few iterations.

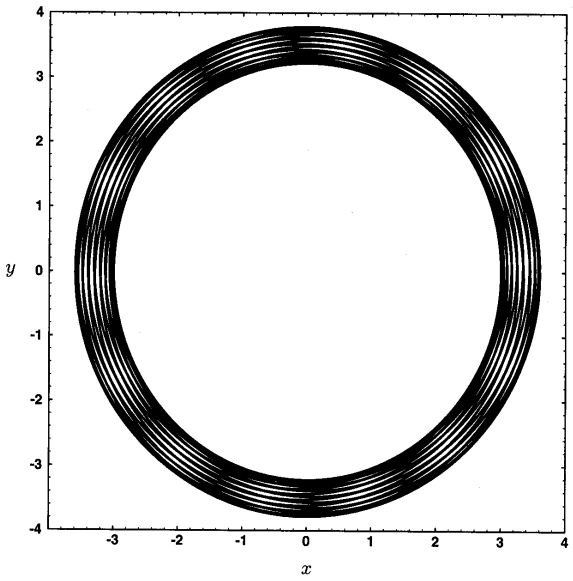


**Fig. 3** A trajectory with initial conditions ($x = 3$, $y = 0$, $u_x = 0$, $u_y = 0.538$).

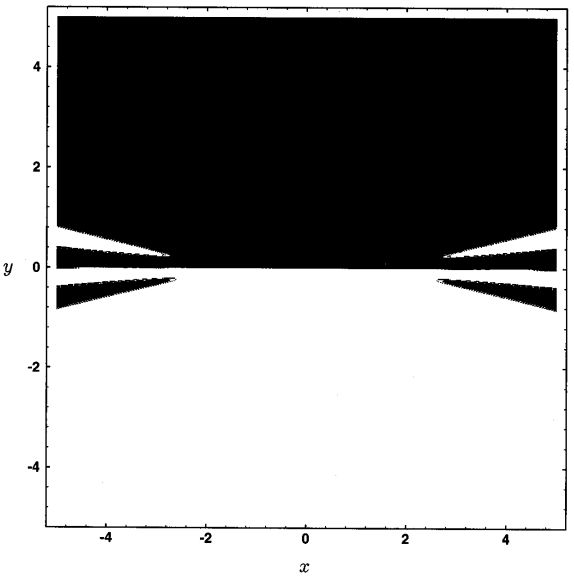


**Fig. 4** A $\mathbf{u} = 0$ section of phase space.

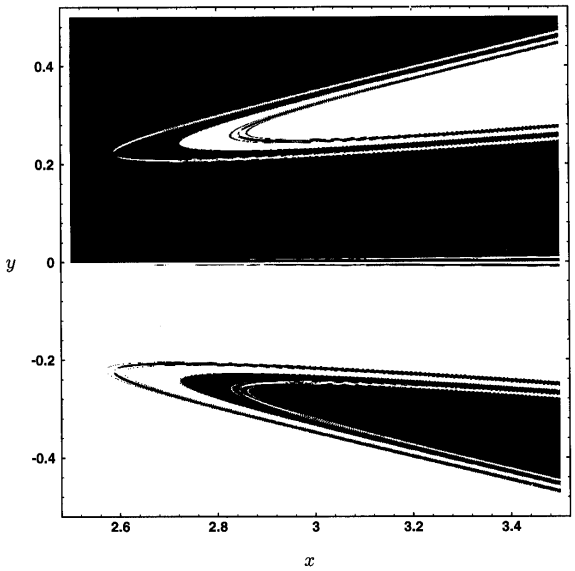


**Fig. 5** A subset of Fig. 4.

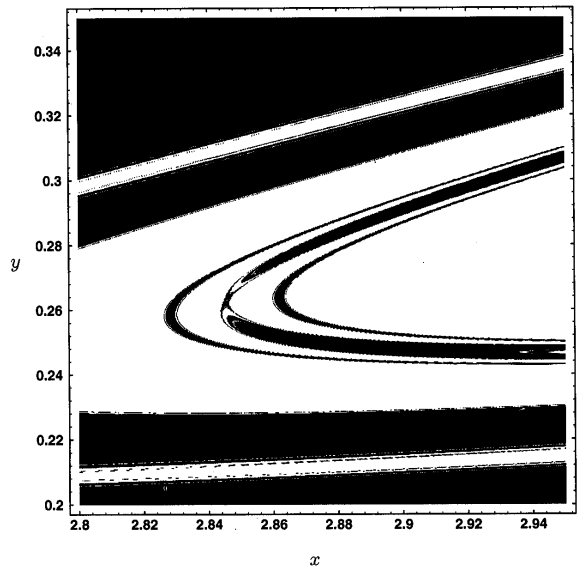


**Fig. 6** A subset of Fig. 5.

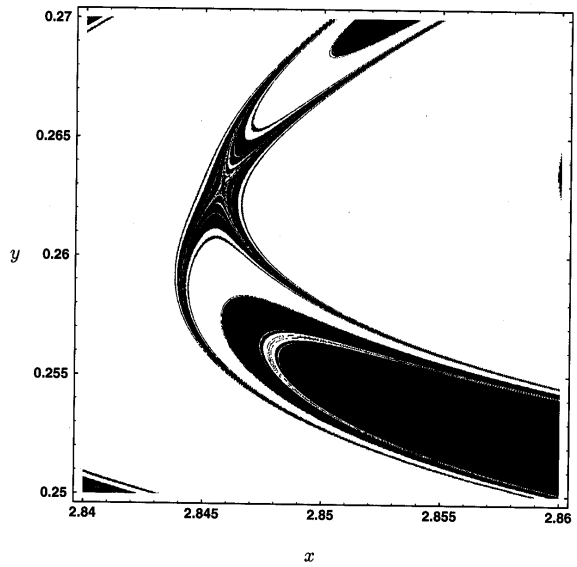


**Fig. 7** A subset of Fig. 6.

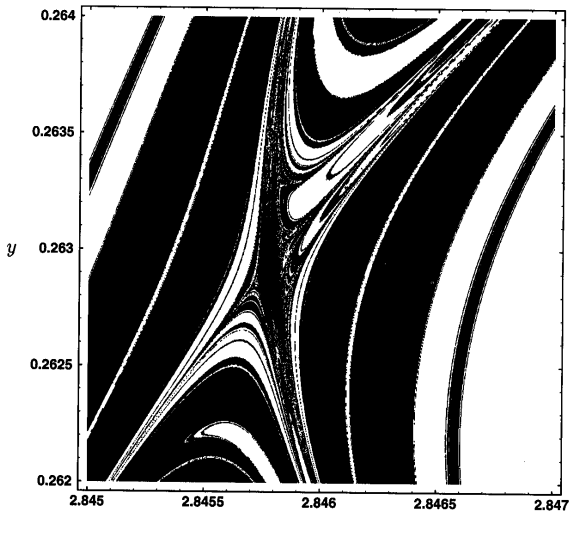


**Fig. 8** A subset of Fig. 7.

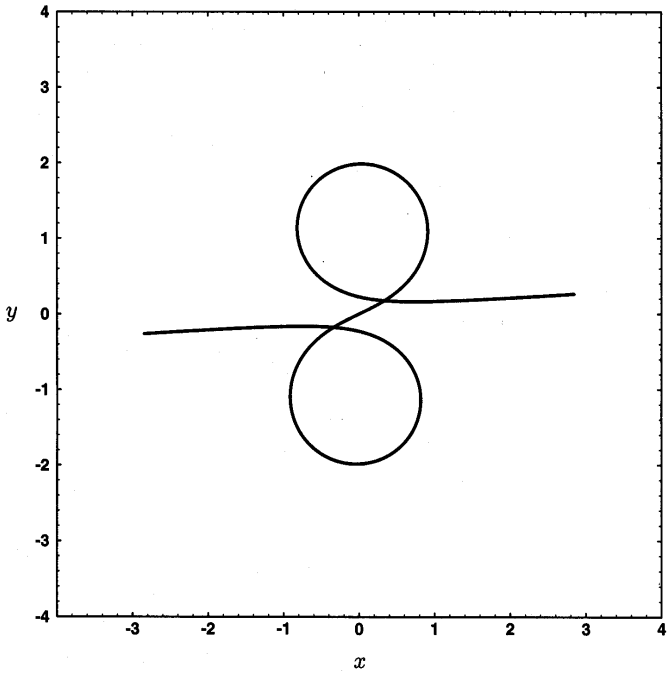


**Fig. 9** A trajectory with initial conditions ($x = 2.8458$, $y = 0.263$, $u_x = 0$, $u_y = 0$).

It does not seem to have been noted in an earlier study of the periodic orbits of this system.[6]

There are a number of parameters which can be modified in the above system. If the charge/mass ratio ($e/m$) is equal to one, there is still a force on a moving test particle, but not on a stationary test particle. Thus the $\mathbf{u} = 0$ section of phase space is all "grey", as none of the particles ever fall into one of the black holes. If it is slightly less than one, however, the result is remarkably similar to that of zero charge, as is evidenced in Fig. 10. With the exception of a slight change of scale and location in phase space, this picture is almost indistinguishable from the equivalent zero charge picture, Fig. 6. This is an example of a form of universality in chaos, where the structure depends only on the topology of orbits in phase space, and not on the detailed form of the equations.

This also means that there are sharp transitions as parameters are varied. For example, if, for $e = 0$, the mass of the black holes is reduced, thus moving towards the nonrelativistic limit, the fractal basins gradually take up more and more of phase space, as the "capture" cross section decreases, until about $M = 0.00602$. At that point, grey regions begin to appear, which eventually take up the whole of phase space, and become the stable orbits which characterize all but a set of zero measure of Newtonian phase space. The phase space for $M = 0.006$ and a typical "Newtonian-like" stable orbit are shown in Figs. 11 and 12. The line for this trajectory is thick because the particle does not follow exactly the same path for each orbit. The is also true of the trajectory shown in Fig. 9, but to a smaller degree.

Also, we may vary the initial velocity. Figures 13–15 show a plot of the $M = 1/3$, $e = 0$ phase space with an initial velocity which is constant over the plot. Note that the boundaries of the grey regions appear to be smooth curves. This is partly explained by the fact that the region in which the total energy is positive is roughly hour-glass shaped.

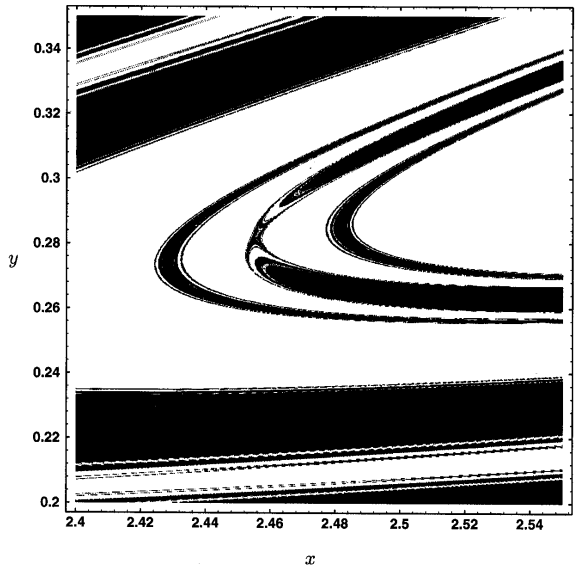


**Fig. 10** A $\mathbf{u} = 0$ section of phase space with $e = 0.99m$.

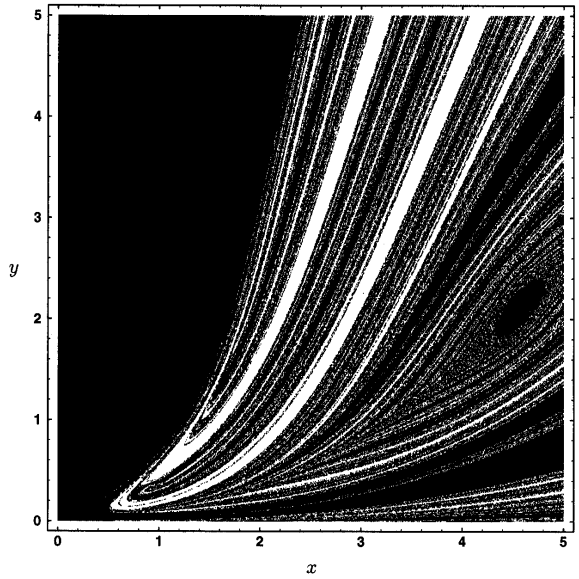


**Fig. 11** A $\mathbf{u} = 0$ section of phase space with $M = 0.006$.

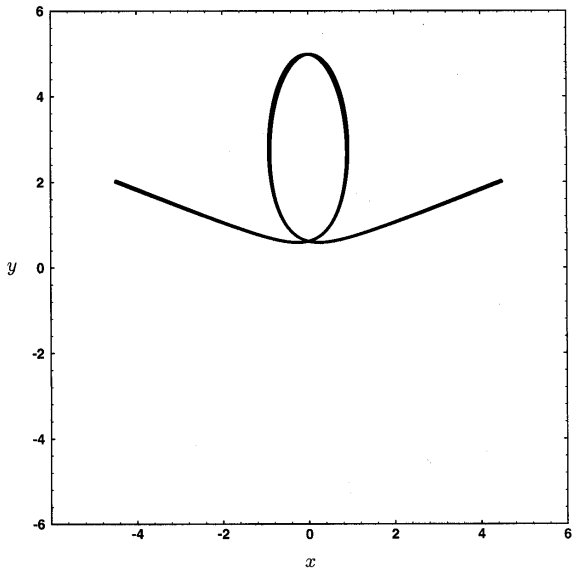


**Fig. 12** A trajectory with $M = 0.006$ and initial conditions ($x = 4.5$, $y = 2$, $u_x = 0$, $u_y = 0$).

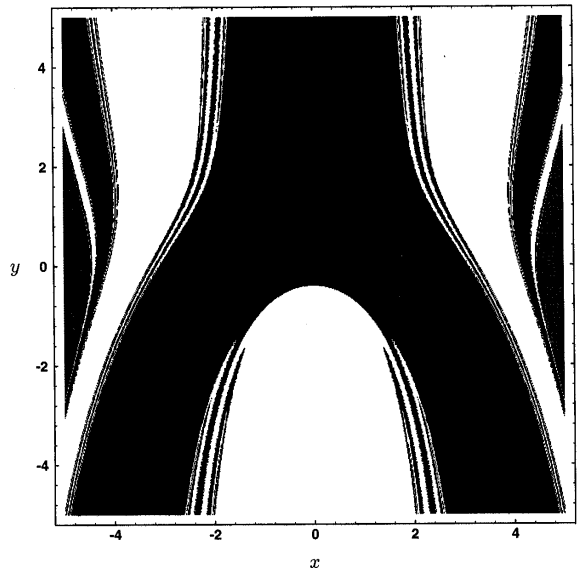


**Fig. 13** A section of phase space with $u_x = 0$, $u_y = 0.4$.

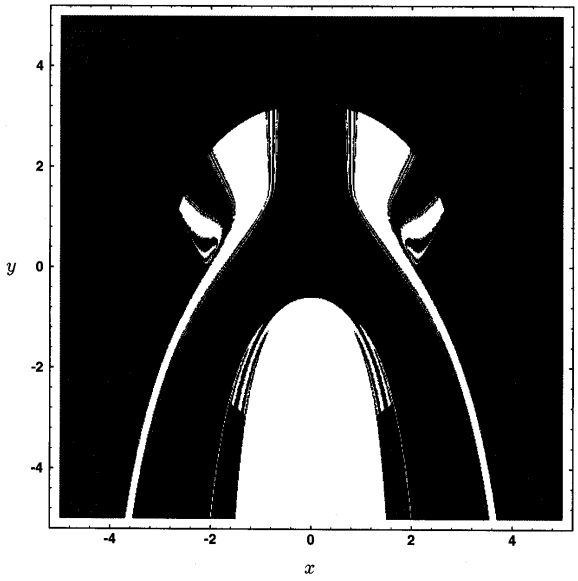


**Fig. 14** A section of phase space with $u_x = 0$, $u_y = 0.7$.

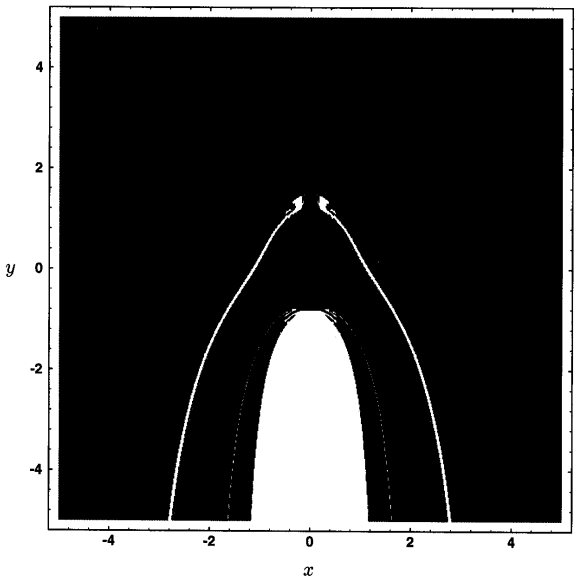


**Fig. 15** A section of phase space with $u_x = 0$, $u_y = 1.5$.

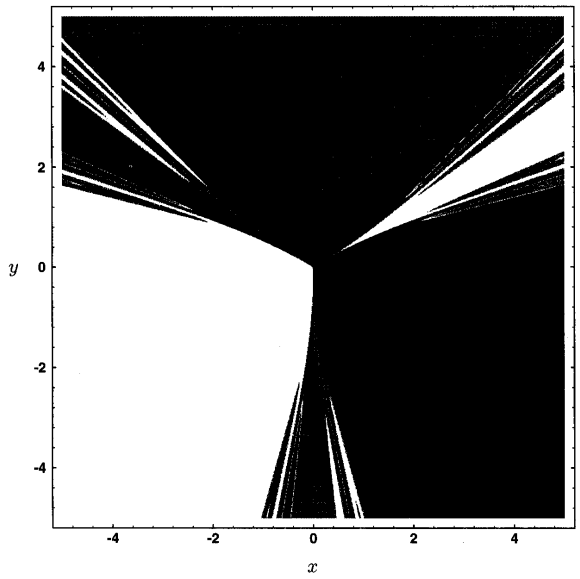


**Fig. 16** A section of three-black-hole phase space with $\mathbf{u} = 0$.

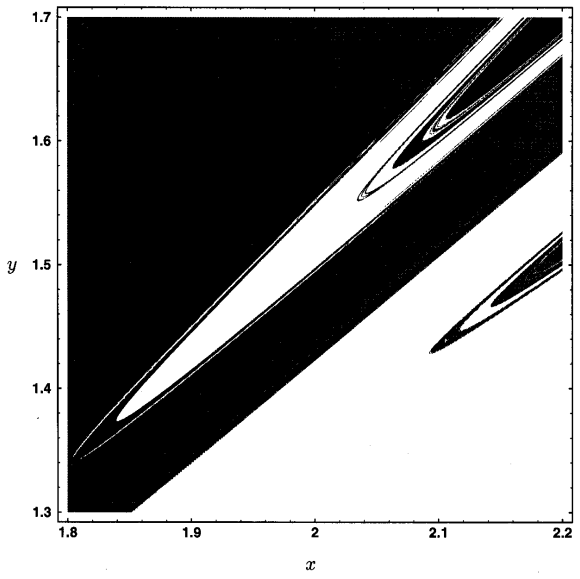


**Fig. 17** A subset of Fig. 16.

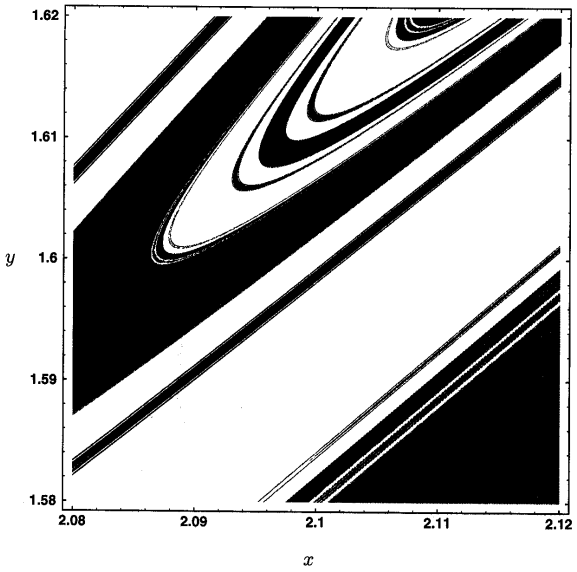


**Fig. 18** A subset of Fig. 17.

The boundary between the basins of attraction still appears to be a fractal.

Finally, we may consider three black holes, as shown in Figs. 16–18. Here, black, white and grey correspond to the basins of attraction of the three holes, which are placed at the vertices of an equilateral triangle of side length $\sqrt{3}$. Each hole has mass 1/3. This section of phase space has the curious feature that between each black and white region there is a grey region, and so on. Or, to put it another way, there is only one basin boundary, and that boundary is the boundary of all three regions. This property is similar to the Julia sets generated by applying Newton's method to cubic equations,[42] and is only possible if the boundary is a fractal. A proof of this property involves an investigation of orbits which just escape falling into a particular black hole. These circle the black hole an infinite number of times, and are arbitrarily close to orbits which circle a large number of times but then escape and head towards either of the other holes. Thus the boundary is arbitrarily close to all three basins of attraction. The Newtonian limit of this system is chaotic, but does not have attractors. A similar nonrelativistic system with attractors and boundary basins is the magnetic pendulum.[43]

## 5. MEASURES OF CHAOS

### 5.1 Fractal Dimensions

There are a number of different fractal dimensions used in the literature.[42,44] The easiest to estimate numerically is the box dimension, which is a non-negative real number assigned to a subset $F$ of $E$-dimensional Euclidean space $R^E$. There are several equivalent definitions. The definition used here to estimate the dimension of the basin boundary numerically is as follows: Fill a section of $R^E$ with a grid of $E$-dimensional cubes of side length $\delta$. Let $N_\delta(F)$ be the number of grid cubes containing $F$. Then the box dimension is:

$$d_B(F) = -\lim_{\delta \to 0} \frac{\ln N_\delta(F)}{\ln \delta} . \qquad (25)$$

Other equivalent definitions include covering the set $F$ with a minimum number of spheres or other shapes or finding the maximum number of disjoint

spheres with centers in $F$. The box dimension involves a limit, so there is no guarantee that it is actually defined for a given set $F$.

If the space is non-Euclidean, for example the curved pseudo-Riemannian spacetime of general relativity, then the concept of a "cube of size $\delta$" in the definition of dimension becomes ill-defined. However it is not necessary to cover the actual fractal object with cubes: Choose a coordinate system, and calculate the box dimension of the object in coordinate space. An important result is that any diffeomorphism, that is, differentiable coordinate transformation, leaves the box dimension invariant, so the original choice of coordinate system was irrelevant, and the box dimension of the object is well defined. Thus we can ignore the curvature of the MP spacetime, and simply calculate the dimension of the basin boundary as if it were embedded in a flat Euclidean space.

The value of $d_B$ was evaluated using the above equation for a region in phase space near that shown in Fig. 6. The region, containing $2520^2$ points, was covered by a grid. Each square of size $\delta$ (a factor of 2520) was counted if it contained points of different color, that is, trajectories with different final outcomes. Figure 19 shows a plot of $\ln N$ vs. $\ln \varepsilon$. The straight line is a least squares fit to all but the three smallest and ten largest values of $\delta$, and gives a dimension of 1.43. The uncertainty is about 0.03, which is typical for such investigations.[45] This uncertainty arises from the sampling of regions in phase space and ambiguity in how to actually perform the fit. The curvature of the graph in Fig. 19 towards small $\delta$ is well explained by the fact that for small box sizes, it is possible to miss a box which actually contains part of the boundary, and hence underestimate $N_\delta$.

The presence of fractal boundary basins indicates that there are non-differentiable (non-smooth) structures in phase space, which implies the system is chaotic. In contrast, an integrable Hamiltonian system has enough constants of motion to determine the motion completely, and these constants must be smooth functions of the phase space coordinates. The usual provisos apply: The numerical methods give estimates of the fractal dimension over a range of scales, but can never take exact $\delta \to 0$ limits. Nevertheless the statement that the boundary is a fractal is quite convincing.

We have performed the same analysis to Fig. 18 for the three-black-hole problem. In this case there are $1260^2$ points, and the resulting graph, leading to a dimension of 1.47, is shown in Fig. 20.

## 5.2 Lyapunov Exponents

Another indicator of chaos for nonrelativistic systems is the presence of positive Lyapunov exponents (defined below) for a non-isolated set of trajectories.

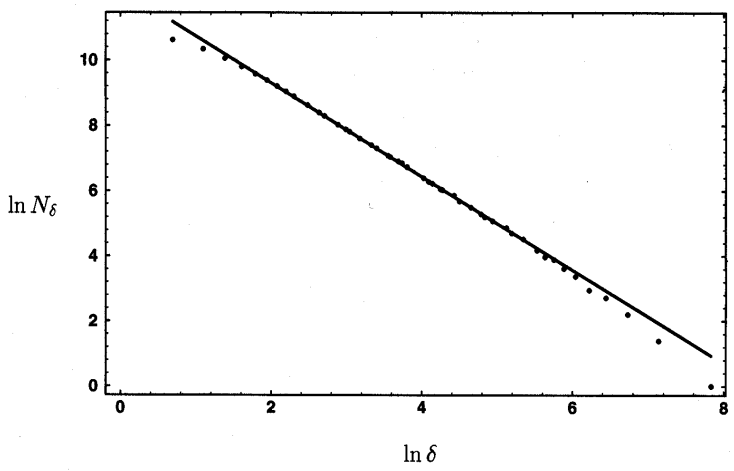


**Fig. 19** The dimension of a section of two-black-hole phase space is 1.43.

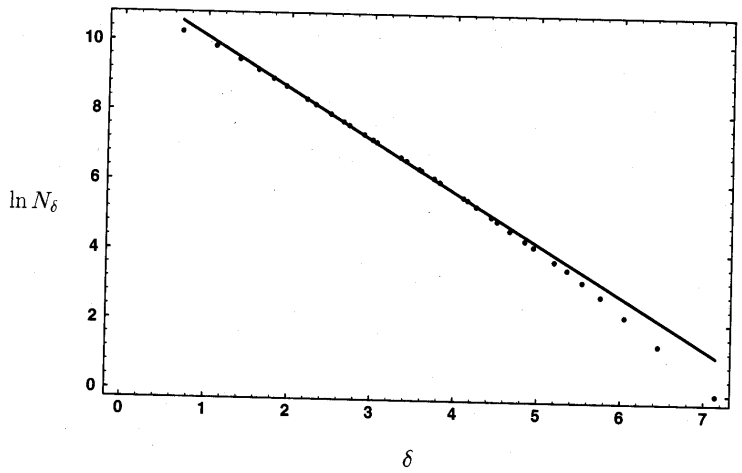


**Fig. 20** The dimension of a section of three-black-hole phase space is 1.47.

The latter condition is necessary because unstable fixed points generally have positive Lyapunov exponents, and occur in integrable as well as chaotic systems. The difference is that the unstable trajectories are isolated in integrable systems, whereas chaotic systems may be composed entirely of unstable trajectories. Typically chaotic systems contain both stable and unstable regions in phase space, with a fractal boundary between the two.

The Lyapunov exponents $\lambda_k$ in flat spacetime are defined by choosing a point $x$ in phase space, at the center of a ball of radius $\varepsilon \ll 1$. After a time $t$ the ball evolves into an ellipsoid with semi-axes $\varepsilon_k(t)$, where $k$ ranges from one to the dimension of the phase space. The Lyapunov exponents are:

$$\lambda_k(x) = \lim_{t\to\infty} \lim_{\varepsilon\to 0} \frac{1}{t} \ln \frac{\varepsilon_k(t)}{\varepsilon}, \qquad (26)$$

assuming the limits exist. The $\lambda_k$ are constant along a trajectory, and are often constant over larger regions of phase space, such as the basin of an attractor.

There are a number of subtleties associated with the definition of Lyapunov exponents in curved spaces, and in particular the MP spacetimes. What time parameter should be used for $t$? This question has particularly plagued the Mixmaster problem, as discussed in Sec. 2. In a general spacetime the only time parameter of any special significance for a trajectory is the proper time $\tau$. If this is used in Eq. (26) the result is a measure of the local instability of phase space trajectories, but does not give information about the global properties of the system. The MP spacetime is static, so that there are a set of distinguished observers "at rest" with respect to the black holes. The time as measured by these observers depends on their position due to the gravitational redshift, but at infinity approaches a constant rate, given by $t$, which appears in the metric, Eq. (1). We will use this parameter, following Ref. 25.

The other difficulty is that it is not obvious how to calculate distances in phase space, given that the original spacetime is curved. Here, as with the fractal dimension, any metric gives the same answers, provided that the trajectory returns arbitrarily close to the starting point, as this causes the metric terms to cancel in the expression $\varepsilon_k(t)/\varepsilon$. The above condition is not very restrictive, as it applies to any trajectories remaining in a compact region of the phase space, including periodic orbits. In our case, this means that Lyapunov exponents are well defined for trajectories which do not fall into a black hole or escape to infinity. In the former case, the limit $t \to \infty$ is also not sensible, while in the latter, the exponents are zero for any metric in phase space which reduces to the special relativistic one in the flat spacetime limit.

The numerical method by which Lyapunov exponents are calculated is described in Ref. 46. For a

general set of coupled ODE's:

$$\dot{x}^i = f^i(\mathbf{x}), \tag{27}$$

the equation for a perturbation $\delta x^i$ is:

$$\delta\dot{x}^i = \delta x^j \frac{\partial}{\partial x^j} f^i(\mathbf{x}), \tag{28}$$

which is a linear equation containing a known function of $\mathbf{x}$, which is unknown. An orthonormal basis of perturbations is integrated at the same time as the equations of motion, and a Gram-Schmidt orthonormalization is carried out periodically to ensure that one vector is lined up in the fastest growing direction, one in the second, and so on; this also ensures that the exponentially growing solutions do not generate overflow or roundoff errors. The Lyapunov exponents are obtained simply by adding the logarithm of the scaling factors in the Gram-Schmidt algorithm, and dividing by the total time. We call this the "straight" algorithm.

In our problem we have the additional difficulty that, in certain regions of phase space, such as those shown in the figures in the previous section, almost all of the trajectories fall into one of the black holes, yet those that do not still have meaningful Lyapunov exponents which we wish to estimate. In an attempt to get around this problem we have used an algorithm which periodically checks whether the trajectory survives a specified time. If it does not, the position in phase space is shifted randomly by a small amount. We have checked that this does not cause the energy to drift perceptibly. The shifting algorithm is difficult to use in that there are a number of parameters to choose, and the shifting routine may fail to find any suitable trajectories. In fact the trajectory given in the table below is the only one we have tried for which it has succeeded for a long integration time. Of course, it gives the same result as the straight algorithm if shifting is not necessary.

It is sometimes possible to calculate Lyapunov exponents analytically. The equations of motion are known, so if an analytic solution for a trajectory can be found, the linear Eq. (28) can be solved, giving a matrix whose eigenvalues are the Lyapunov exponents. One such trajectory is the unstable fixed point midway between the black holes.

For the general case of a fixed point, $U_{,i} = 0$, where $i$ indicates $x$ or $y$, and the comma is a partial derivative, as usual. The linearized equations become

$$\frac{d}{d\tau}\begin{pmatrix}\delta x\\ \delta y\\ \delta u_x\\ \delta u_y\end{pmatrix} = \begin{pmatrix}0 & 0 & U^{-1} & 0\\ 0 & 0 & 0 & U^{-1}\\ aU_{,xx} & aU_{,xy} & 0 & 0\\ aU_{,xy} & aU_{,yy} & 0 & 0\end{pmatrix} \times \begin{pmatrix}\delta x\\ \delta y\\ \delta u_x\\ \delta u_y\end{pmatrix}, \tag{29}$$

with

$$a = \frac{1}{U^2}\left(1 - \frac{e}{m}\right), \tag{30}$$

and have solutions of the form $e^{l\tau}$ where $l$ is an eigenvalue of the above matrix, that is,

$$l = \pm\sqrt{\frac{1-e/m}{2U^3}} \times \sqrt{U_{,xx}+U_{,yy} \pm \sqrt{(U_{,xx}-U_{,yy})^2+4U_{,xy}^2}}\,. \tag{31}$$

The Lyapunov exponents are closely related to the values of $l$, but differ in the following ways: An imaginary value of $l$ leads to oscillatory solutions which have Lyapunov exponent zero, and the exponents are calculated using the global time $t$, so that the remaining exponents are given by $\lambda = U^{-1}l$, using the metric Eq. (1). Thus the Lyapunov exponents may be calculated for a fixed point, and depend only on the values of $U$ and its derivatives at the point, and the value of $e/m$. The analytic value for the fixed point in the case of two black holes of mass 1/3 is given in Table 1, and agrees with the numerically evaluated result to five significant figures.

If $e = m$, the above expression yields zero for the Lyapunov exponents, which can be understood physically because the force on the particle is proportional to $v^2$ for small $v$, so the equations linearized about the stationary solution are trivial. These analytic values are useful in checking the numerics, but do not yield any information about the chaos, since they apply to trajectories which are not in chaotic regions.

The trajectories which have been integrated numerically in Table 1 are the unstable fixed point at the origin, which compares very closely with the analytic result; the trajectory plotted in Fig. 3; the

**Table 1 Lyapunov Exponents for the Two-Black-Hole Problem**

| Initial Conditions | Algorithm | $\lambda_1$ | $\lambda_2$ | $\lambda_3$ | $\lambda_4$ |
|---|---|---|---|---|---|
| (0, 0, 0, 0) | Analytic | $\frac{18}{25\sqrt{5}}$ | 0 | 0 | $-\frac{18}{25\sqrt{5}}$ |
| (0, 0, 0, 0) | Straight | 0.32199 | 0.00001 | −0.00001 | −0.32199 |
| (3, 0, 0, 0.538) | Straight | 0.00007 | 0.00002 | −0.00001 | −0.00007 |
| (2.8458, 0.263, 0, 0) | Straight | 0.00005 | 0.00000 | −0.00001 | −0.00003 |
| (3, 0, 0, 0) | Straight | 0.11222 | 0.00007 | −0.00007 | −0.11222 |
| (3.33467, 0.23509, 0, 0) | Shifting | 0.03609 | 0.00006 | −0.00006 | −0.03609 |

trajectory plotted in Fig. 9; a trajectory which oscillates up and down the $x$-axis; and a trajectory "on" the boundary which has needed to be shifted. All of these have been integrated for $t = 10^5$ time units. The "algorithm" is either the analytic calculation given above, the straight algorithm, or the shifting algorithm.

It is clear that the numerical results reflect the symmetries of the equations. The sum of the exponents is zero, due to Liouville's theorem. In addition, two of the exponents are (approximately) zero due to the one constant of motion $E$. As the length of the integration increases, these decrease, showing that they are due to the finite averages used, and not the numerical errors in the equations.

Two of the orbits appear to have all four exponents zero. This is expected, since they are numerically stable in that a small perturbation of the initial conditions does not cause a qualitative difference in the trajectory.

The trajectory which oscillates along the $x$-axis is in the unusual position of being exactly calculable (in theory: the result is a complicated integral), but arbitrarily close to the fractal boundary. See Fig. 5. It is only a special orbit in that the integration can be carried on for an indefinite time due to the symmetry of the equations. Otherwise it is similar to the other unstable periodic orbits of this system. It might be possible to analyze the Lyapunov exponents of this system by noting that an arbitrary point on the basin boundary is arbitrarily close to periodic orbits. The Lyapunov exponents for the periodic orbits could be evaluated with some definiteness, because only a finite time is required.

## 6. DISCUSSION

We have seen that there are difficulties in applying the standard tests of chaos to general relativistic systems. Because the spacetime and the phase space derived from it depend on an arbitrary choice of coordinate system, quantities which depend on distances in phase space, such as Lyapunov exponents become poorly defined and unsuitable as a test for chaos. For the MP problem, the spacetime is static, so a natural global time variable exists, and these problems become less severe. In any case, quantities which are topological in nature, or at least coordinate independent, such as the fractal nature of structures in phase space, are equally good for relativistic problems. Poincare sections also fall into this category.

The motion of particles in systems of two or three fixed black holes exhibits many of the features common to non-relativistic chaotic systems, such as sensitive dependence on initial conditions leading to nonzero Lyapunov exponents and fractal basin boundaries. There are islands of stability hidden in the chaos. The structure of the phase space depends only slightly on the charge of the particle. What is unusual about this problem is the presence of attractors in a non-dissipative system. The fractal boundaries of the basins of these attractors are particularly useful to quantify the chaos, since their dimension does not depend on the chosen coordinate system.

Since the two black hole problem has an integrable Newtonian limit, it should be possible to observe the break up of the KAM tori explicitly as the mass of the black holes is increased from zero. What makes this limit most interesting is that the

relativistic effects lead to capture of the particle, a process that is not present in the non-relativistic system.

In closing, we remark that fractal geometry is particularly well suited to studying chaos in the most geometrical of theories — general relativity.

## REFERENCES


1. J. Wisdom, *Icarus* **72**, 241 (1987).
2. J. Wisdom, *Proc. R. Soc. London* **A413**, 109 (1987).
3. P. Carruthers, *Astrophys. J.* **380**, 24 (1991).
4. G. Contopoulos, *Proc. R. Soc. London* **A431**, 183 (1990).
5. G. Contopoulos, *Proc. R. Soc. London* **A435**, 551 (1991).
6. G. Contopoulos and H. Papadaki, *Celest. Mech. Dyn. Astron.* **55**, 47 (1993).
7. C. P. Dettmann, N. E. Frankel and N. J. Cornish, *Phys. Rev.* **D50**, R618 (1994).
8. C. W. Misner, *Phys. Rev. Lett.* **22**, 1071 (1969).
9. V. A. Belinskii, E. M. Lifshitz and I. M. Khalatnikov, *Usp. Fiz. Nauk* **102**, 463 (1970). [*Sov. Phys. Usp.* **13**, 745 (1971)].
10. A. B. Burd, N. Buric and G. F. R. Ellis, *Gen. Relativ. Gravit.* **22**, 349 (1990).
11. S. E. Rugh and B. J. T. Jones, *Phys. Lett.* **A147**, 353 (1990).
12. D. Hobill et al., *Class. Quantum Grav.* **8**, 1155 (1991).
13. J. D. Barrow, *Phys. Rep.* **85**, 1 (1982).
14. I. M. Khalatnikov et al., *J. Stat. Phys.* **38**, 97 (1985).
15. A. B. Burd, N. Buric and R. K. Tavakol, *Class. Quantum Grav.* **8**, 123 (1991).
16. P. D. B. Collins and E. J. Squires, *Found. Phys.* **23**, 913–921 (1993).
17. M. Szylowski, J. Szczęsny and M. Biesiada, *Chaos Solitons Fractals* **1**, 233 (1991).
18. M. Szylowski, *Phys. Lett.* **A176**, 22 (1993).
19. U. Yurtsever, preprint gr-qc-9412031 submitted to *Phys. Rev. D* (1994).
20. A. Burd and R. Tavakol, *Phys. Rev.* **D47**, 5336 (1993).
21. J. Koiller, J. R. T. De Mello Neto and I. Damião Soares, *Phys. Lett.* **A110**, 260 (1985).
22. E. Calzetta and C. El Hasi, *Class. Quantum Grav.* **10**, 1825 (1993).
23. H. Varvoglis and D. Papadopoulos, *Astron. Astrophys.* **261**, 664 (1992).
24. L. Bombelli and E. Calzetta, *Class. Quantum Grav.* **9**, 2573 (1992).
25. V. Karas and D. Vokrouhlický, *Gen. Relativ. Gravit.* **24**, 729 (1992).
26. Proceedings of the NATO ARW "Deterministic Chaos in General Relativity" eds., A. Burd, A. Coley and D. Hobill (Plenum, New York, 1994).
27. *Chaos Solitons Fractals* **4**(3), "Quantum Mechanics and Chaotic Fractals," eds., S. El Naschie and O. E. Rossler (1994).
28. S. D. Majumdar, *Phys. Rev.* **72**, 390 (1947).
29. A. Papapetrou, *Proc. R. Irish Acad.* **A51**, 191 (1947).
30. J. B. Hartle and S. W. Hawking, *Commun. Math. Phys.* **26**, 87 (1972).
31. C. P. Dettmann and N. E. Frankel, *J. Stat. Phys.* **72**, 241 (1993).
32. C. J. S. Clarke, *Class. Quantum Grav.* **11**, 1375 (1994).
33. D. Kastor and J. Traschen, *Phys. Rev.* **D47**, 5370 (1993).
34. D. R. Brill et al., *Phys. Rev.* **D49**, 840 (1994).
35. C. W. Misner, K. S. Thorne and J. A. Wheeler, *Gravitation* 897 (Freeman, New York, 1973).
36. H. Goldstein, *Classical Mechanics* (Addison-Wesley, Reading, 1980).
37. B. Carter, *Phys. Rev.* **174**, 1559 (1968).
38. S. Chandrasekhar, *Proc. R. Soc. London* **A421**, 227 (1989).
39. N. C. A. da Costa, F. A. Doria and A. F. Furtado do Amaral, *Int. J. Theor. Phys.* **32**, 2187 (1993).
40. V. I. Arnold and A. Avez, *Ergodic Problems of Classical Mechanics* (Benjamin, New York, 1968).
41. W. H. Press et al., *Numerical Recipes in C* (Cambridge University Press, Cambridge, 1988).
42. K. Falconer, *Fractal Geometry and its Applications* (Wiley, Chichester, 1990).
43. S. McDonald et al., *Physica* **D17**, 125 (1985).
44. B. B. Mandelbrot, *The Fractal Geometry of Nature* (Freeman, New York, 1977).
45. M. Obert, *Fractals* **1**, 711 (1993).
46. I. Shimada and T. Nagashima, *Prog. Theor. Phys.* **61**, 1605 (1979).